International Journal of Nanomedicine

Dovepress
open access to scientific and medical research

Open Access Full Text Article

ORIGINAL RESEARCH

Angiogenesis and bone regeneration of porous nano-hydroxyapatite/coralline blocks coated with rhVEGF$_{165}$ in critical-size alveolar bone defects in vivo

This article was published in the following Dove Press journal:
International Journal of Nanomedicine
31 March 2015
Number of times this article has been viewed

Bing Du[1,2]
Weizhen Liu[1]
Yue Deng[1,3]
Shaobing Li[1]
Xiangning Liu[4]
Yan Gao[1]
Lei Zhou[1]

[1]Department of Oral Implantology, Guangdong Provincial Stomatological Hospital, Southern Medical University, Guangzhou, People's Republic of China; [2]Center of Stomatology, The First People's Hospital of Foshan, Foshan, Guangdong, People's Republic of China; [3]Department of Oral and Maxillofacial Surgery, Qingdao Stomatological Hospital, Qingdao, People's Republic of China; [4]Department of Stomatology, The First Affiliated Hospital of Jinan University, Guangzhou, People's Republic of China

Abstract: To improve the regenerative performance of nano-hydroxyapatite/coralline (nHA/coral) block grafting in a canine mandibular critical-size defect model, nHA/coral blocks were coated with recombinant human vascular endothelial growth factor$_{165}$ (rhVEGF) via physical adsorption (3 μg rhVEGF$_{165}$ per nHA/coral block). After the nHA/coral blocks and VEGF/nHA/coral blocks were randomly implanted into the mandibular box-shaped defects in a split-mouth design, the healing process was evaluated by histological observation and histomorphometric and immunohistological analyses. The histological evaluations revealed the ingrowth of newly formed blood vessels and bone at the periphery and cores of the blocks in both groups at both 3 and 8 weeks postsurgery, respectively. In the histomorphometric analysis, the VEGF/nHA/coral group exhibited a larger quantity of new bone formation at 3 and 8 weeks postsurgery. The percentages of newly formed bone within the entire blocks in the VEGF/nHA/coral group were 27.3%±8.1% and 39.3%±12.8% at 3 weeks and 8 weeks, respectively, and these values were slightly greater than those of the nHA/coral group (21.7%±3.0% and 32.6%±10.3%, respectively), but the differences were not significant ($P>0.05$). The immunohistological evaluations revealed that the neovascular density in the VEGF/nHA/coral group (146±32.9 vessel/mm^2) was much greater than that in the nHA/coral group (105±51.8 vessel/mm^2) at the 3-week time point ($P<0.05$), but no significant difference was observed at the 8-week time point (341±86.1 and 269±50.7 vessel/mm^2, respectively, $P>0.05$). The present study indicated that nHA/coral blocks might be optimal scaffolds for block grafting in critical-size mandibular defects and that additional VEGF coating via physical adsorption can promote angiogenesis in the early stage of bone healing, which suggests that prevascularized nHA/coral blocks have significant potential as a bioactive material for bone regeneration in large-scale alveolar defects.

Keywords: angiogenesis, bone regeneration, tissue engineering, block grafting, nano-hydroxyapatite/coralline, critical size, bone defect

Introduction

Clinically, large alveolar defects caused by periodontal disease, tumor, trauma, or surgery are challenging in dentistry.[1,2] Although alveolar bones have the capability to regenerate, the healing process frequently fails to progress through the normal stages of healing or is delayed when the defects reach a critical size.[3–5] Therefore, bone grafting is necessary for large defects.

Currently, autogenous grafts are considered the gold standard for bone regeneration due to their osteogenic potential, osteoinductivity, and osteoconductivity.[6–8] However, such grafts have yet to be applied clinically due to donor site limitations, morbidity, and

Correspondence: Lei Zhou
Department of Oral Implantology, Guangdong Provincial Stomatological Hospital, Southern Medical University, Guangzhou, GuangDong, 510280, People's Republic of China
Tel +86 20 8423 3801
Fax +86 20 8443 3177
Email zho668@263.net

additional injury. In contrast, xenogenic block grafts are commercially available, free from size constraints, and result in less morbidity at the harvest site. Additionally, these grafts can easily be fabricated into suitable grafts for bone defects.

In tissue engineering, the scaffolds are of critical importance.[9–11] Optimal design of scaffolds should mimic the extracellular matrix in chemical components and micro- and macrostructure and be beneficial to the promotion of cell adhesion, migration, and proliferation. Additionally, scaffolds can also act as carriers for growth factors with biological properties, such as bone morphogenetic proteins (BMPs) and vascular endothelial growth factor (VEGF).[12,13]

Coralline hydroxyapatite (CHA) is one of the synthetic porous biomaterials among numerous xenogenous grafting materials and is made by partially converting calcium carbonate from coral to a hydroxyapatite (HA) layer on the surface via a hydrothermal exchange. CHA is a composite scaffold with an outer HA layer and an inner coralline core.[14] Numerous experiments have demonstrated that the space between CHA particles is enveloped by cells and collagen matrix and occupied by new bone.[15] Moreover, CHA particles have exhibited good performance in increasing initial periodontal ligament cell attachment in periodontal regeneration.[16] Therefore, CHA particles have been widely used clinically in periodontal and implant surgery due to their favorable osteogenic effects.[17] However, predictable results have not been achieved in bone regeneration with particle grafts, due to their weakness in shape remodeling.[18] In comparison, HA/coral blocks might be advantageous for maintaining space and rebuilding bone volume. Unfortunately, bone formation with CHA blocks offers a lower capacity for osteogenesis than that provided by particles.[19] At present, autogenous blocks and xenogenic particles are more widely used than xenogenic blocks in the restoration of critical-size alveolar defects. Indeed, there are still few reports of CHA block grafting for alveolar defects. Therefore, the vascularization and osteogenesis of block grafts remain a key problem for dentists.

Importantly, the healing ability of bone relies on the recruitment of progenitor cells and neovascularization at the injury site. Thus, the promotion of angiogenesis and prevascularization of the scaffolds achieved by coating them with angiogenic growth factors might be one of the most viable approaches for bone construction in critical-size defects.[20] Recombinant human vascular endothelial growth factor$_{165}$ (rhVEGF$_{165}$) is a potent and widely used angiogenic growth factor that is well known to induce the migration, proliferation, and differentiation of vascular endothelial cells, to control their apoptosis, and to improve new vessel formation.[21,22] rhVEGF$_{165}$ also has the capabilities to upregulate the expression of BMP-2 and enhance new bone formation.[23]

To prevascularize block grafts and enhance the formation of new blood vessels and bones, we coated nano-hydroxyapatite (nHA)/coral blocks with rhVEGF$_{165}$ and investigated the angiogenesis and the bone regenerative performances of bio-coated and pure nHA/coral blocks in critical-size mandibular defects in dogs. This study might provide theoretical support for the clinical application of nHA/coral block grafts. In this study, we made the following hypotheses: 1) nHA/coral blocks might act as optimal scaffolds for new bone formation and vessels in critical-size mandibular defects, and 2) nHA/coral coated with rhVEGF$_{165}$ might improve angiogenesis and new bone formation.

Materials and methods

Scaffold characterization

The nHA/coral scaffolds used in this study were supplied by Beijing YHJ Science and Trade Co., Ltd (Beijing, People's Republic of China). The scaffold blocks (6×9×12 mm^3) were sterilised by γ-irradiation before use. The morphologies of their surfaces and cores were analyzed with JSM-6300 scanning electron microscopy (SEM) (Jeol Co., Ltd, Tokyo, Japan) at 20 kV. The dried samples were coated with gold–palladium under an argon atmosphere. SEM photomicrographs were used to analyze the pore sizes and crystal diameters.

Animals

The four male beagle dogs (age 12–15 months; mean weight 12.1±0.5 kg) used in the study were provided by the Guangdong Provincial Medical Experimental Animal Center (licence number: SYXK [yue] 2012-0081). Rabies vaccinations, vermifuge treatments, and overall examinations were completed prior to the experiments. All animals exhibited healthy and permanent dentition. In the experiment, the animals were independently housed in box-type cages (1.0×1.0×1.0 m) and fed once per day with a soft food diet and water. The experimental work began after an adaptation period of 1 week. Additionally, the ethical committee of the Guangdong Provincial Stomatological Hospital approved the animal experimental protocol. Supplemental information about the experimental animals: rabies vaccinations, vermifuge treatments, and overall examinations, including alanine aminotransferase, aspartate amino transferase, alkaline phosphatase, total protein, albumin, urea nitrogen, creatinine, glucose, total cholesterol, total bilirubin, white

blood cell, red blood cell (RBC), hemoglobin concentration, mean RBC volume, mean hemoglobin concentration of RBC, platelet, platelet distribution width, mean platelet volume, were completed prior to the experiments. Additionally, the animals in the experiment were independently housed in box-type cages (1.0×1.0×1.0 m) in general housing facilities. After the operations, milk was given for extra nutrition for 3 days.

Study design and grouping

The study was performed in two surgical phases. In the first phase, the bilateral mandibular second, third, and fourth premolars and the first and second molars (P2–M2) were extracted from each dog. After the tooth extractions, four standardized box-shaped defects were surgically created at the buccal aspect of the alveolar ridge in each mandible (n=8). Following 2 months of submerged healing, the chronic-type defects were reshaped and randomly allocated in a split-mouth design to the nHA/coral group or the VEGF/nHA/coral group. Uncoated nHA/coral blocks served as controls. Accordingly, all dogs received each treatment procedure once. The animals were sacrificed after a submerged healing period of 3 or 8 weeks. (Supplemental information about animal group allocation and study design: There were two groups in our study, the VEGF/nHA/coral group [ie, the experimental group] and the nHA/coral group [ie, the control group]. The animals were randomly chosen for the experiments. Additionally, the defects were divided into nHA/coral and VEGF/nHA/coral sites in a split-mouth design.)

Anesthesia protocol

Prior to the surgical procedures, the dogs were fasted overnight and handled according to the following anesthesia protocol. After intramuscular sedation with sumian xin (composition: 2,4-dimethylaniline thiazole, ethylenediamine tetra acetic acid, dihydroetorphine hydrochloride, and haloperidol; 0.2 mL/kg body weight; Animal Husbandry Research Institute, Jilin, People's Republic of China), anesthesia was induced by intravenous injection of 3% pentobarbital solution (0.3 mL/kg body weight; Foshan Chemical Engineering Experimental Factory, Foshan, People's Republic of China). Prior to the surgery, primacaine (0.2 mL/kg body weight; Merignac Cedex, France) was injected locally into the surgical area of the mandible. Additionally, intramuscular benzylpenicillin (Longteng pharmaceutical company, Sichuan, People's Republic of China; 80×10^6 U/d) was given intra- and postoperatively to each animal for 7 days.

Surgical phase 1 (tooth extraction and defect creation)

In the first surgery, after reflection of full-thickness flaps, the bilateral P2–M2 molars were removed from the mandible with minimal trauma in each dog. After tooth extraction, four standardized box-type defects (9 mm in height from the crestal bone, 6 mm in depth from the surface of the buccal bone, and 12 mm in width mesiodistally) were created in the buccal bone at a distance of 4 mm with carbide burs as previously reported.[24] The corresponding lingual bone plates were left intact (Figure 1A). All osteotomy procedures were performed under adequate irrigation with sterile 0.9% physiological saline. The wounds were closed with interrupted mattress sutures (Foosin Medical Supplies Inc., Weihai, People's Republic of China). All sites were allowed to heal for 2 months.

Soak loading of the nHA/coral blocks

For the soak loading of the nHA/coral blocks, the growth factor rhVEGF$_{165}$ (PeproTech) was dissolved in sterile saline in aseptic conditions. Each block was incubated with 0.25 mL of 12 μg/mL rhVEGF$_{165}$ solution (3 μg rhVEGF$_{165}$ per block).[25] The control samples were incubated with 0.25 mL of sterile saline as previously reported.[26] All blocks were implanted within 30 minutes of assembly.

Surgical phase 2 (bone grafting)

In the second surgery, bilateral vestibular incisions were made, and mucoperiosteal flaps were reflected to expose the sites for block grafting in the lower jaws (Figure 1B). Prior to grafting, the chronic-type defects were reshaped (6×9×12 mm) with carbide burs, and all defects were grouped into either the nHA/coral block or the nHA/coral block soaked with rhVEGF$_{165}$ group in a split-mouth design (Figure 1C). Following periosteal-releasing incisions, the mucoperiosteal flaps were repositioned coronally and closed with interrupted mattress sutures (Foosin; Medical Supplies Inc.) for a submerged healing period of 3 or 8 weeks.

Histological observation/ histomorphometric analysis

After 3 or 8 weeks, the animals were sacrificed with an overdose of anesthetic. The lower jaws were detached and placed in 4% neutral buffered formalin solution. Seven days later, the jaws were dissected with a carborundum disk, and each experimental specimen contained one block and the surrounding bone tissue.

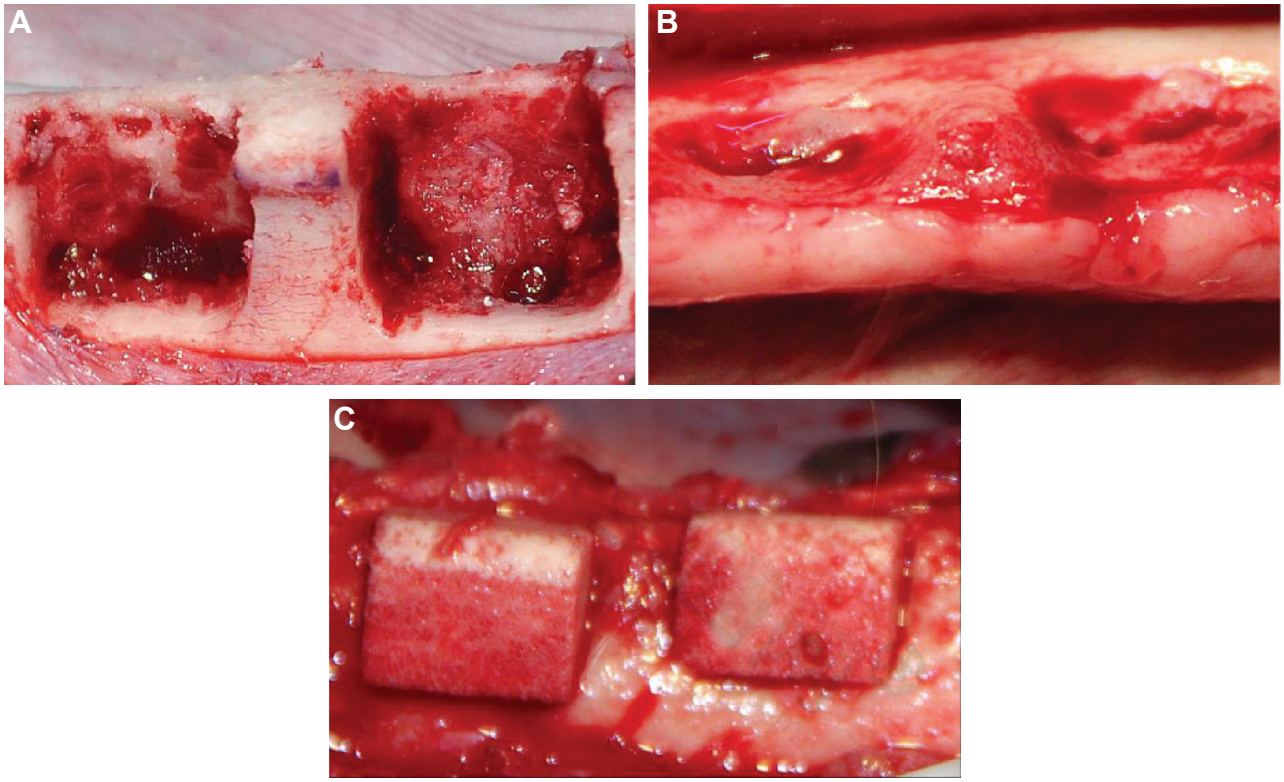

Figure 1 (**A**) Standardized box-type defects (9 mm in height from the crestal bone, 6 mm in depth from the surface of the buccal bone, and 12 mm in width mesiodistally; distance between defects: 4 mm). The defects were surgically created at the buccal aspect of the alveolar ridge after tooth extraction in the lower jaws (buccal view). (**B**) A chronic-type defect morphology was achieved after 2 months of submerged healing (occlusal view). (**C**) After defect reshaping, nano-hydroxyapatite/coralline blocks were grafted to fill the defect sites (buccal view).

The samples were decalcified in 10% ethylenediaminetetraacetic acid, dehydrated using ascending concentrations of alcohol, and paraffin embedded. The samples were sectioned at 5 μm thickness and stained with hematoxylin and eosin (Figure 2A) and Masson trichrome. Each of the three sections per sample was evaluated separately by two blinded observers using a digital microscope (BX51, Olympus Co., Tokyo, Japan) and a digital camera (DP71, Olympus) at 10× magnification (Figure 2B). The entire scaffold and the newly formed bone within each block were then outlined (Figure 2C) and measured with the Image-Pro Plus image analysis software (Media Cybernetics, Carlsbad, CA, USA). The percentages of new bone fill (PBF = newly formed bone area/the entire scaffold area) were measured. Masson trichrome-stained sections were used to define the collagen secreted in the process of bone formation as an indirect index of the quantity of the newly formed bone.

Immunohistological staining

After decalcification, hydration, paraffin embedding, and sectioning (5 μm), slides from independent samples harvested at 3 and 8 weeks were immunostained for the von Willebrand factor (vWF), which is a protein present in large quantities in subendothelial matrices such as blood vessel basement membranes.[27] All processes were performed following the manufacturer's protocol using a rabbit antidog vWF primary antibody (1:1,500) and biotinylated antirabbit immunoglobulin G from a commercial kit (Abcam, Cambridge, UK) and followed by counterstaining with hematoxylin. All slides were imaged with an Olympus BX51 light microscope and an Olympus DP71 digital camera. The positively stained blood vessels were counted manually at 200× magnification within the scaffold area, and blood vessel density was calculated using the Image-Pro Plus Software (Media Cybernetics) as previously reported.[25]

Statistical analyses

All data are expressed as the mean ± the standard deviation (n=8). The statistical analyses were performed with SPSS 18.0 (SPSS Inc., Chicago, IL, USA). Independent-sample *t*-tests were used to analyze the significance of the differences between groups and between the different time

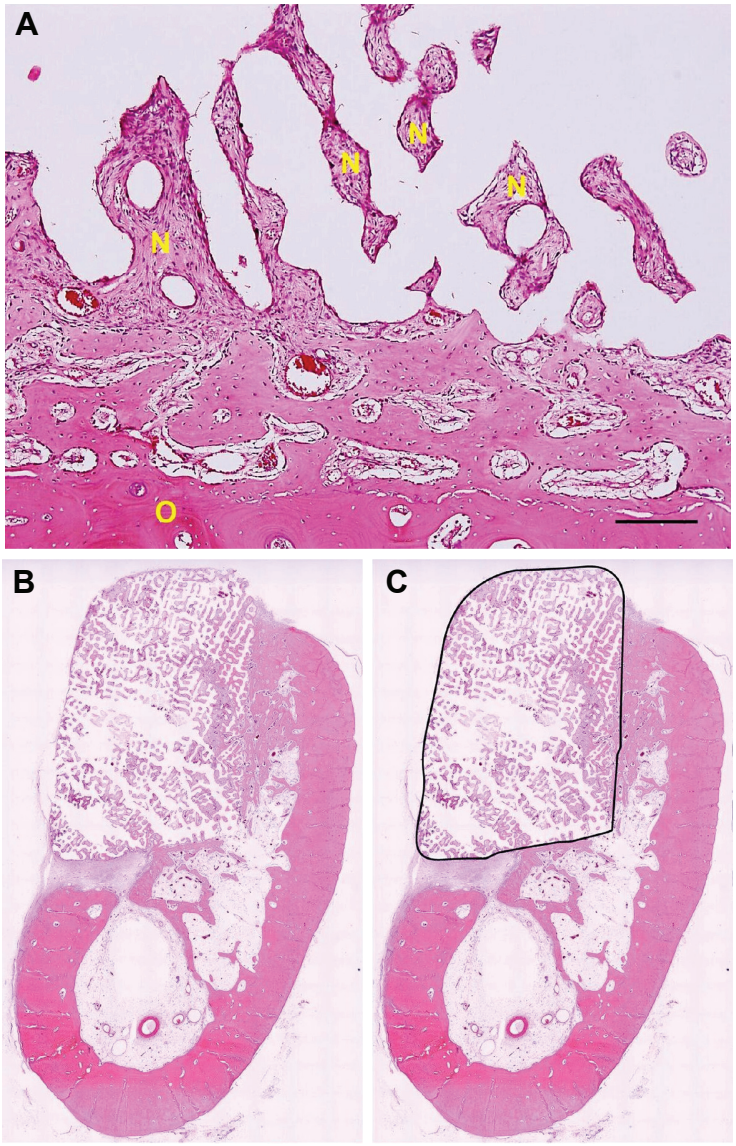

Figure 2 A section stained by hematoxylin and eosin: O=old bone; N=new bone; bar: 200 μm (**A**). Decalcified sections implanted with two scaffolds. Upon sacrifice at 3 or 8 weeks, each defect was removed with the surrounding tissue, buccolingually sectioned, and stained with hematoxylin and eosin (**B**). The total scaffold area (black line) was quantified using Image-Pro Plus software; the new bone was traced, and the percentage of new bone fill was determined based on the size of the entire scaffold area (**C**).

points within groups, and the level of significance was set at $P<0.05$.

Results

Scaffold presentation and morphology

The nHA/coral blocks were three-dimensionally porous generally (Figure 3A). The porous structures were visualized with SEM (Figure 3B). The pore sizes ranged from 57 μm to 164 μm. All macropores inside the block were in spatial communication via interconnected pores. The diameters of the interconnected pores varied from 107 μm to 550 μm. The hydroxyapatite (HA) crystals were well distributed on the surface and had diameters that varied from 71 nm to 99 nm (Figure 3C).

Histological observations/ histomorphometric analysis

In general, the postoperative healing was uneventful in all animals. No complications such as swelling, premature exposure of the grafting sites, and infections were observed throughout the entire study period.

In both groups, the neovascular tissues and newly formed bone were observed on the surface and in the macropores at the four peripheral parts of the blocks at 3 weeks after

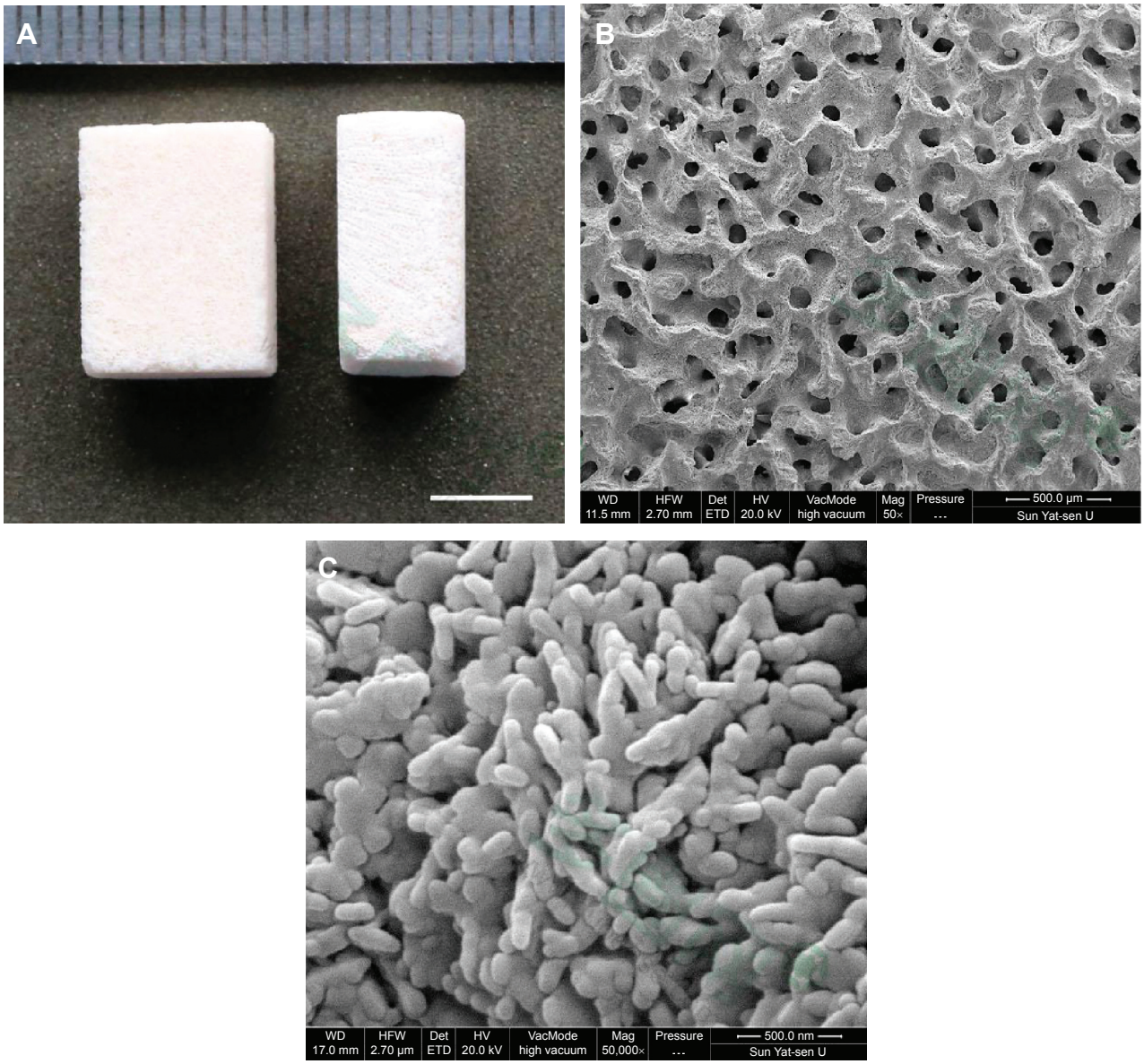

Figure 3 Cross-sectional view of the porous nano-hydroxyapatite/coralline block, scale bar: 5 mm (**A**). The interconnected pore system of the scaffold was visualized and measured with scanning electron microscopy (**B**) Nano-scaled hydroxyapatite crystals were found on the surface by scanning electron microscopy (**C**).

surgery. Additionally, the newly formed bone and blood vessels had grown toward the centers between macropores through the interconnecting paths. Moreover, the lines of the active osteoblasts and collagen were observed in the macropores at the peripheral parts of the scaffolds; new bone was seldom found in the centers of the blocks in either group. The shapes of the blank areas and the newly formed bone were regular. Furthermore, histomorphometric analyses revealed that the PBFs were 21.7%±3.0% and 27.3%±8.1% in the nHA/coral group and VEGF/nHA/coral group, respectively. The quantity of newly formed bone in the VEGF/nHA/coral group was slightly more than that in the nHA/coral group; however, no significant increase with respect to PBF was observed after coating the nHA/coral blocks with VEGF ($P>0.05$, Figure 4).

Eight weeks after surgery, the macropores at the periphery adjacent to the host bone and the center were filled with interconnected newly formed bone in both groups. Compared with the sample taken at 3 weeks, the structure of the trabecular bone in the peripheral parts had increased in width, and considerable amounts of woven bone and new blood vessels were present in the peripheral parts adjacent to the host bone. The shapes of the blank areas and the newly formed bone were still regular. Additionally, at 8 weeks, the PBFs were 32.6%±10.3% for the blank sample and 39.3%±12.8% for the VEGF sample. Compared with

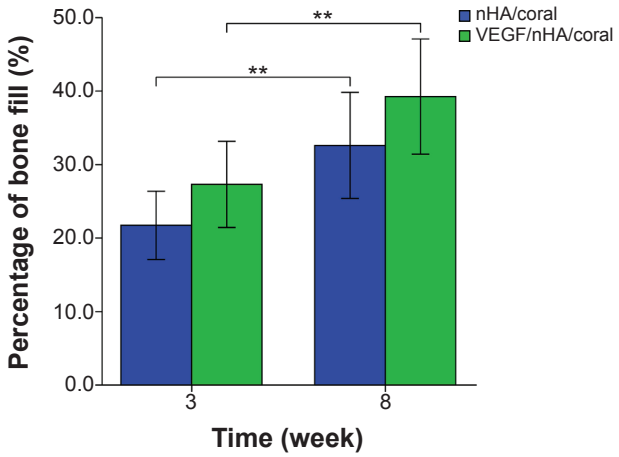

Figure 4 Histomorphometric analysis of the newly formed bone. The columns indicate the mean values, and the error bars represent the corresponding standard deviations (n=8).
Note: **$P<0.01$.
Abbreviations: nHA/coral, nano-hydroxyapatite/coralline; VEGF, vascular endothelial growth factor.

week 3, the PBFs at week 8 were significantly increased in both the VEGF/nHA/coral ($P<0.01$) and nHA/coral groups ($P<0.01$). Additionally, the quantity of newly formed bone in the VEGF/nHA/coral group was greater than that in the nHA/coral group; however, no significant increase in PBF was to be observed after coating the nHA/coral blocks with VEGF ($P>0.05$; Figure 4).

From the Masson staining images, collagen expression could be observed in terms of blue-stained tissue. At 3-week time point, collagen as the most important component of bone matrix was secreted copiously, with collagen fibers connected together to form the tabular structure as the matrix of mineralization in both groups. In addition, lines of active osteoblasts were observed around the tabular bone and a large number of neovascular channels can be easily found, especially in VEGF/nHA/coral group (Figure 5A). As the time point increased to 8 weeks, collagen progressively increased along with the new bone formation. Moreover, the mineralization degree of newly formed tabular structures increased significantly in both groups (Figure 5B).

Immunohistochemical analysis

Immunohistochemical analysis revealed that the formation of new blood vessels was characterized by the vWF staining of numerous endothelial cells located in the vessel basement membranes (Figure 6A). The uneven distribution of the newly formed blood vessels was easily observed. The neovascular structure at the periphery, adjacent to the host bone, was more evident than that at the center of the sample. At the 3-week time point, compared with the nHA/coral block group (105±51.8 vessel/mm^2), an increase in new blood vessel density was evident after in the combined nHA/coral block with VEGF group (146±32.9 vessel/mm^2, $P<0.05$). The neovascular density within the scaffolds in the VEGF/nHA/coral block group was significantly increased ($P<0.05$). At the later 8-week time point, the neovascular densities of both groups had significantly increased ($P<0.01$). At the 8-week time point, the neovascular densities increased to 269±50.7 vessel/mm^2 in the nHA/coral block group and 341±86.1 vessel/mm^2 in the VEGF/nHA/coral block group, and there was no significant difference between the two groups ($P>0.05$) (Figure 6B).

Discussion

Bone healing in critical-size alveolar defects requires different grafting approaches to greatly improve volume and

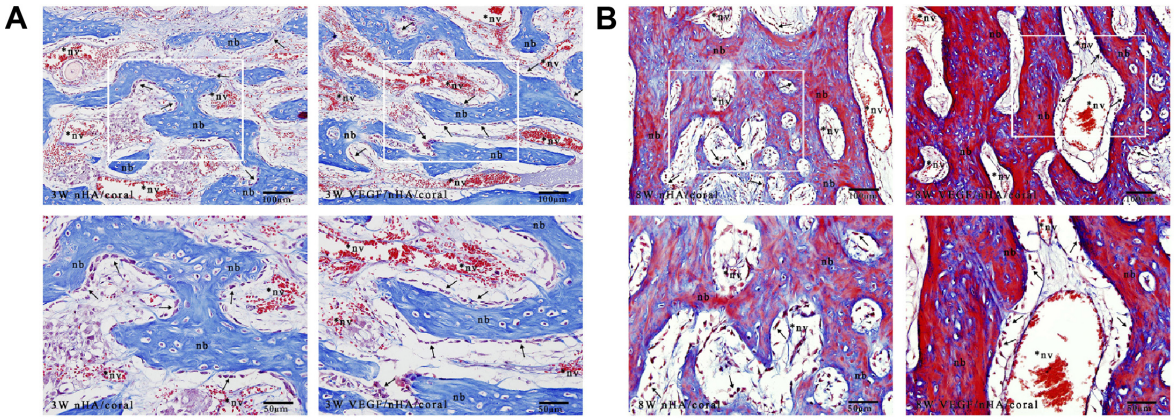

Figure 5 Histological observation of the Masson staining.
Notes: Representative images showing the expression of collagen (stained in blue), newly formed blood vessels (nv), new tabular bone (nb), and lines of osteoblasts (black arrows) within the scaffolds of both groups at different time points. (**A**) Represents the masson stained section at the timepoint of 3 weeks; (**B**) represents the masson stained section at the timepoint of 8 weeks.

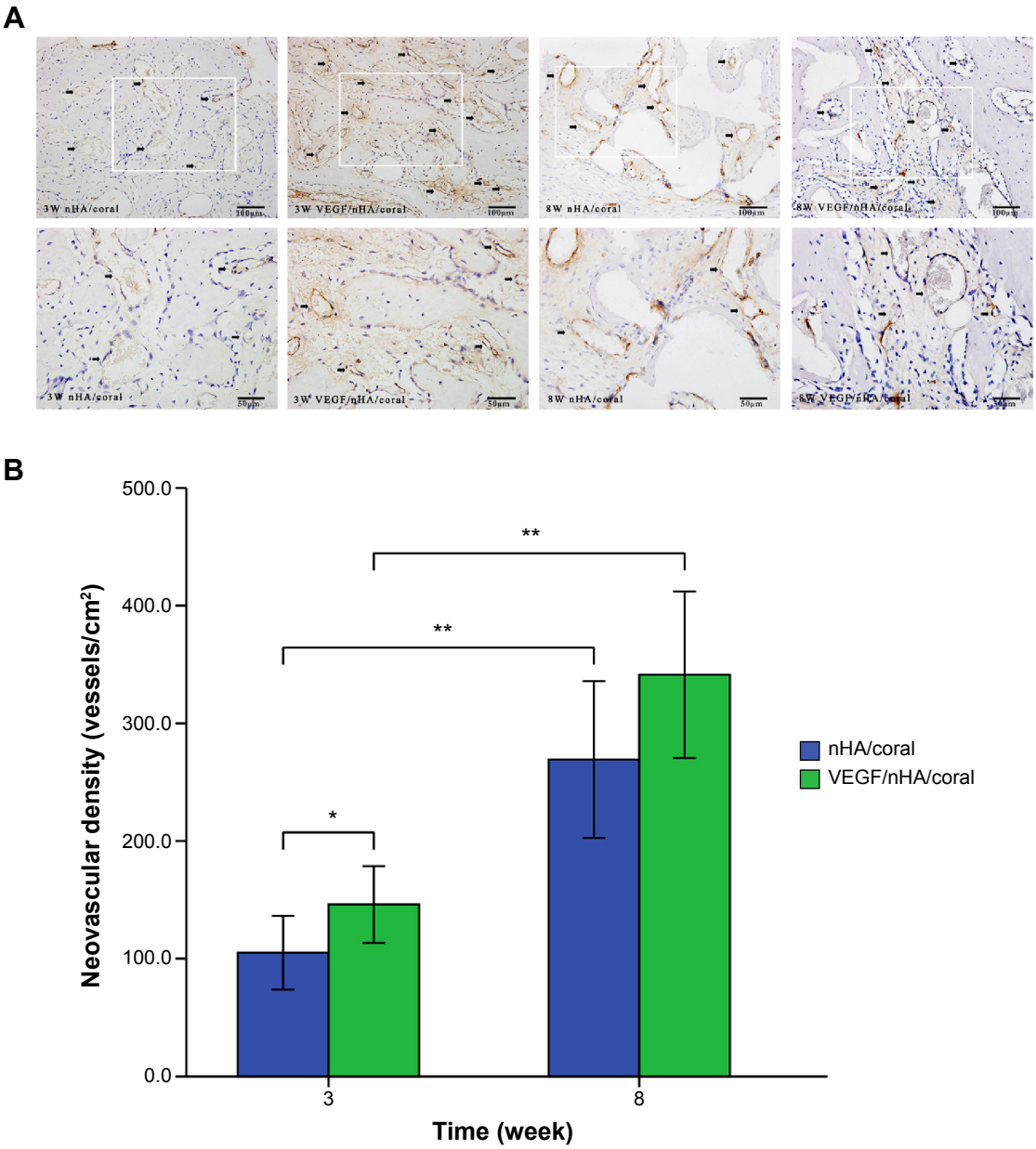

Figure 6 Staining for vWF of the decalcified tissues treated with nHA/coral blocks.
Notes: (**A**) Representative images of the nHA/coral and VEGF/nHA/coral groups showing circular, dark brown vessels (black arrows) in the scaffolds. The VEGF/nHA/coral group displayed greater densities of new blood vessels than the nHA/coral group at each time point. (**B**) The blood vessel densities were calculated based on the immunohistochemical staining. The VEGF released from the scaffolds promoted the formation of new blood vessels. The columns indicate the mean values, and the error bars represent the corresponding standard deviations (n=8). *$P<0.05$; **$P<0.01$.
Abbreviations: vWF, von Willebrand factor; nHA/coral, nano-hydroxyapatite/coralline; VEGF, vascular endothelial growth factor.

shape. The data presented in our study support the notion that optimal scaffold grafting can result in good performance in terms of new bone regeneration, and that combinatorial approaches involving the local delivery of angiogenic growth factors from scaffolds can provide significant therapeutic benefits.

In bone tissue engineering, the pore sizes and interconnectivities of the pores in the scaffold play important roles in blood vessel growth, the migration of cells, and bone formation.[28] Some studies have reported that the aggregated space between the pores acts as the passageway for the metabolism of cells and the transportation of nutrition that promote the ingrowth of blood vessels.[29–31] Yoshikawa et al[32] suggested that the pore size in grafts used for bone healing should be at least 50 μm. Larger pore sizes result in greater quantities of nutrition and oxygen being transported into the inside of the scaffold.[29] Moreover, scaffolds with larger pore sizes provide more superficial area and improve cell adhesion

and proliferation due to full contact between the graft and body fluids.[31,33,34] However, Grynpas et al[33] noted that oversized pores not only reduce mechanical strength but also influence cell function and new bone formation. High levels of interconnectivity between the pores enhance the porosity and enlarge the superficial area and consequently increase the numbers of endothelial cells and active osteoblasts.[35,36] It is important to note that our histological evidence revealed obvious cell migration from the peripheries to the cores of the nHA/coral blocks at the 3-week time point; collagen matrices were also readily observable in the centers. There were more newly formed blood vessels and greater quantities of bone tissue present at the 8-week time point. These results indicate that the nHA/coral blocks had excellent characteristics in terms of biocompatibility, pore size, and pore interconnectivity and were able to provide appropriate interconnected paths for cell migration and bone regeneration.

The vWF immunostaining results indicated a significant increase in neovascularization due to the use of the nHA/coral blocks combined with VEGF at 3 weeks and revealed no significant improvement in vascular density at 8 weeks; these findings demonstrated the excellent effect of VEGF local therapy in terms of angiogenesis at an early stage of bone repair. Interestingly, the areas of newly formed bone in the VEGF/nHA/coral group at 3 and 8 weeks were slightly greater than those of the blank scaffold group; however, there were no significant differences in PBF between the two groups. Some previous studies have demonstrated that bioactive glass combined with VEGF can participate in bone healing through indirect processes, and these findings accord well with the well correlated results of the present study. Specifically, the enhancements of angiogenesis and bone maturation are involved in these processes, whereas osteoprogenitor differentiation and bone formation are not.[25] At the 8-week time point, the quantities of new bone tissue had continuously increased in the peripheries and centers of the blocks in both groups. A slightly greater amount of new bone formation was observed in the VEGF/nHA/coral group, but there was no significant difference in PBF between the two groups. The results from our study demonstrated that local VEGF therapy delivered by combining nHA/coral blocks and VEGF might only improve neovascularization in the early stage and not significantly increase bone regeneration.

In previous experiments, several methods have been developed to coat scaffolds with growth factors for bone tissue engineering. Fu et al[37] utilized CHA and poly(lactic-co-glycolic acid) microspheres encapsulated BMP-2, that were fabricated with the water-in-oil-in-water (w/o/w) double-emulsion method as carriers for BMP. Shiels et al's[38] experiments have illustrated that rhBMP-2 can be bound to the surface of HA either by direct physical adsorption or via a polyelectrolyte coating. In our study, the nHA/coral blocks were infused with VEGF$_{165}$ via a direct adsorption approach as previously reported.[26] We chose this method for the following reasons. First, this method is simple and practical for animal studies and clinical operation. Second, this method does not require freeze-drying or a second sterilization to protect the scaffold's bioactivity. Third, some studies have suggested that three types of functional groups in the HA crystals – ie, –OH, –NH_2, and –$COOH^-$ groups – can interact with protein molecules via noncovalent adsorption.[39] Last, porous surfaces such as those created by the surface of the porous nanostructured HA crystals on the nHA/coral blocks provide more functional groups for the adsorption of growth factors. However, Mizushima et al[40] reported that proteins and drugs are rapidly released from HA based on an in vitro study, and this speed of release was unsatisfactory. In our immunohistochemical and histomorphometric analyses, only angiogenesis in the early stage was improved by the physical resorption of VEGF onto the nHA/coral block. No significant increase in osteogenesis was noted in the VEGF/nHA/coral group, which demonstrated that the function of VEGF was not continuously and completely developed. At 3 and 8 weeks, uneven distributions of new bone and blood vessels between the peripheries and cores of the scaffolds were observed in both groups. These findings are signs of insufficient blood, oxygen, and nutrient supplies in the cores of scaffolds. Previous experiments have revealed that uneven nutrition and oxygen supplies are likely to occur to some degree when the volume of the defect is increased and the oxygen concentrations in the cores of large-scale blocks are significantly decreased in the cell culture.[41] The gradient diffusion of oxygen and nutrients might influence cellular proliferation and differentiation within block grafts and consequently influence bone formation.

Therefore, many types of composite scaffold systems, such as HA/gelatine and nHA/chitsan, have been developed and successfully applied in bone tissue engineering to achieve sustained release.[42,43] Some experiments have demonstrated that different doses and dual delivery of VEGF and BMP-2 might lead to different effects on bone regeneration.[44] A previous study reported that the combination of gradient VEGF with BMP-2 and Wnt released from a three-dimensional biodegradable porous calcium phosphate scaffold can promote

angiogenesis and bone formation more readily than a single factor alone.[45]

Hence, in bone tissue regeneration, local therapies with different doses of single or combinations of growth factors result in complicated in vivo cascades that involve the presence of clots containing large numbers of mesenchymal cells followed by high proliferative and metabolic levels in osteoblasts and macrophages and the formation of vascular structures and woven bone. Hence, in our ongoing work, we plan to develop a multilayer biodegradable composite scaffold and to optimize the growth factor dose, other possible cytokine combinations, and their controlled release.

Conclusion

Our results indicate that the nHA/coral block is an optimal scaffold for block grafting with an ideal mesoporous structure and nanosized HA crystals. The characterizations performed in vivo demonstrated that porous nHA/coral blocks coated with $rhVEGF_{165}$ promoted neovascularization in the early stage of bone healing but failed to enhance bone formation. VEGF/nHA/coral blocks might serve as potential biological scaffolds for improving bone regeneration in orthopedic and implant surgeries.

Acknowledgments

This work was supported by the Guangdong Provincial Stomatological Hospital (Southern Medical University, People's Republic of China), grants from the Natural Science Foundation of China (No 81170998), and the Fund of Guangdong Province Medical Science Research (C2012034).

Disclosure

The authors report no conflicts of interest related to this work.

References

1. Polimeni G, Susin C, Wikesjo UM. Regenerative potential and healing dynamics of the periodontium: a critical-size supra-alveolar periodontal defect study. *J Clin Periodontol.* 2009;36:258–264.
2. Lee J, Tran Q, Seeba G, Wikesjo UM, Susin C. The critical-size supraalveolar peri-implant defect model: reproducibility in histometric data acquisition of alveolar bone formation and osseointegration. *J Clin Periodontol.* 2009;36:1067–1074.
3. Xu L, Lv K, Zhang W, Zhang X, Jiang X, Zhang F. The healing of critical-size calvarial bone defects in rat with rhPDGF-BB, BMSCs, and beta-TCP scaffolds. *J Mater Sci Mater Med.* 2012;23:1073–1084.
4. Guo J, Meng Z, Chen G, et al. Restoration of critical-size defects in the rabbit mandible using porous nanohydroxyapatite-polyamide scaffolds. *Tissue Eng Part A.* 2012;18:1239–1252.
5. Rentsch C, Rentsch B, Breier A, et al. Long-bone critical-size defects treated with tissue-engineered polycaprolactone-co-lactide scaffolds: a pilot study on rats. *J Biomed Mater Res A.* 2010;95:964–972.
6. Mokbel N, Bou SC, Matni G, Naaman N. Healing patterns of critical size bony defects in rat following bone graft. *Oral Maxillofac Surg.* 2008;12:73–78.
7. Inoda H, Yamamoto G, Hattori T. rh-BMP2-induced ectopic bone for grafting critical size defects: a preliminary histological evaluation in rat calvariae. *Int J Oral Maxillofac Surg.* 2007;36:39–44.
8. Yazdi FK, Mostaghni E, Moghadam SA, Faghihi S, Monabati A, Amid R. A comparison of the healing capabilities of various grafting materials in critical-size defects in guinea pig calvaria. *Int J Oral Maxillofac Implants*. 2013;28:1370–1376.
9. Keogh MB, O'Brien F, Daly JS. A novel collagen scaffold supports human osteogenesis – applications for bone tissue engineering. *Cell Tissue Res.* 2010;340:169–177.
10. Rodrigues CV, Serricella P, Linhares AB, et al. Characterization of a bovine collagen-hydroxyapatite composite scaffold for bone tissue engineering. *Biomaterials*. 2003;24:4987–4997.
11. Kong L, Ao Q, Wang A, et al. Preparation and characterization of a multilayer biomimetic scaffold for bone tissue engineering. *J Biomater Appl.* 2007;22:223–239.
12. Matsuo T, Sugita T, Kubo T, Yasunaga Y, Ochi M, Murakami T. Injectable magnetic liposomes as a novel carrier of recombinant human BMP-2 for bone formation in a rat bone-defect model. *J Biomed Mater Res A*. 2003;66:747–754.
13. Ozturk BY, Inci I, Egri S, et al. The treatment of segmental bone defects in rabbit tibiae with vascular endothelial growth factor (VEGF)-loaded gelatin/hydroxyapatite "cryogel" scaffold. *Eur J Orthop Surg Traumatol*. 2013;23:767–774.
14. Koeter S, Tigchelaar SJ, Farla P, Driessen L, van Kampen A, Buma P. Coralline hydroxyapatite is a suitable bone graft substitute in an intra-articular goat defect model. *J Biomed Mater Res B Appl Biomater*. 2009;90:116–122.
15. Koo KT, Polimeni G, Qahash M, Kim CK, Wikesjo UM. Periodontal repair in dogs: guided tissue regeneration enhances bone formation in sites implanted with a coral-derived calcium carbonate biomaterial. *J Clin Periodontol.* 2005;32:104–110.
16. Devecioglu D, Tozum TF, Sengun D, Nohutcu RM. Biomaterials in periodontal regenerative surgery: effects of cryopreserved bone, commercially available coral, demineralized freeze-dried dentin, and cementum on periodontal ligament fibroblasts and osteoblasts. *J Biomater Appl.* 2004;19:107–120.
17. Yilmaz S, Kuru B. A regenerative approach to the treatment of severe osseous defects: report of an early onset periodontitis case. *Periodontal Clin Investig*. 1996;18:13–16.
18. Wikesjo UM, Lim WH, Razi SS, et al. Periodontal repair in dogs: a bioabsorbable calcium carbonate coral implant enhances space provision for alveolar bone regeneration in conjunction with guided tissue regeneration. *J Periodontol*. 2003;74:957–964.
19. de Macedo NL, de Macedo LG, Matuda FS, Ouchi SM, Monteiro AS, Carvalho YR. Guided bone regeneration with subperiosteal implants of PTFE and hydroxyapatite physical barriers in rats. *Braz Dent J*. 2003;14:119–124.
20. Poh CK, Ng S, Lim TY, Tan HC, Loo J, Wang W. In vitro characterizations of mesoporous hydroxyapatite as a controlled release delivery device for VEGF in orthopedic applications. *J Biomed Mater Res A*. 2012; 100:3143–3150.
21. Yang P, Wang C, Shi Z, et al. rhVEGF 165 delivered in a porous beta-tricalcium phosphate scaffold accelerates bridging of critical-sized defects in rabbit radii. *J Biomed Mater Res A.* 2010;92:626–640.
22. Lode A, Wolf-Brandstetter C, Reinstorf A, et al. Calcium phosphate bone cements, functionalized with VEGF: release kinetics and biological activity. *J Biomed Mater Res A.* 2007;81:474–483.
23. Street J, Bao M, DeGuzman L, et al. Vascular endothelial growth factor stimulates bone repair by promoting angiogenesis and bone turnover. *Proc Natl Acad Sci U S A*. 2002;99:9656–9661.
24. Schwarz F, Ferrari D, Balic E, Buser D, Becker J, Sager M. Lateral ridge augmentation using equine- and bovine-derived cancellous bone blocks: a feasibility study in dogs. *Clin Oral Implants Res.* 2010;21: 904–912.

25. Leach JK, Kaigler D, Wang Z, Krebsbach PH, Mooney DJ. Coating of VEGF-releasing scaffolds with bioactive glass for angiogenesis and bone regeneration. *Biomaterials*. 2006;27:3249–3255.
26. Schwarz F, Rothamel D, Herten M, Ferrari D, Sager M, Becker J. Lateral ridge augmentation using particulated or block bone substitutes biocoated with rhGDF-5 and rhBMP-2: an immunohistochemical study in dogs. *Clin Oral Implants Res*. 2008;19:642–652.
27. Xiao C, Zhou H, Liu G, et al. Bone marrow stromal cells with a combined expression of BMP-2 and VEGF-165 enhanced bone regeneration. *Biomed Mater*. 2011;6:015013.
28. Holy CE, Fialkov JA, Davies JE, Shoichet MS. Use of a biomimetic strategy to engineer bone. *J Biomed Mater Res A*. 2003;65:447–453.
29. Cyster LA, Grant DM, Howdle SM, et al. The influence of dispersant concentration on the pore morphology of hydroxyapatite ceramics for bone tissue engineering. *Biomaterials*. 2005;26:697–702.
30. Karageorgiou V, Kaplan D. Porosity of 3D biomaterial scaffolds and osteogenesis. *Biomaterials*. 2005;26:5474–5491.
31. Moreau JL, Xu HH. Mesenchymal stem cell proliferation and differentiation on an injectable calcium phosphate-chitosan composite scaffold. *Biomaterials*. 2009;30:2675–2682.
32. Yoshikawa T, Nakajima H, Uemura T, et al. In vitro bone formation induced by immunosuppressive agent tacrolimus hydrate (FK506). *Tissue Eng*. 2005;11:609–617.
33. Grynpas MD, Pilliar RM, Kandel RA, Renlund R, Filiaggi M, Dumitriu M. Porous calcium polyphosphate scaffolds for bone substitute applications in vivo studies. *Biomaterials*. 2002;23:2063–2070.
34. Klenke FM, Liu Y, Yuan H, Hunziker EB, Siebenrock KA, Hofstetter W. Impact of pore size on the vascularization and osseointegration of ceramic bone substitutes in vivo. *J Biomed Mater Res A*. 2008;85:777–786.
35. Roy TD, Simon JL, Ricci JL, et al. Performance of degradable composite bone repair products made via three-dimensional fabrication techniques. *Biomed Mater Res A*. 2003;66:283–291.
36. Kruyt MC, de Bruijn JD, Wilson CE, et al. Viable osteogenic cells are obligatory for tissue-engineered ectopic bone formation in goats. *Tissue Eng*. 2003;9:327–336.
37. Fu K, Xu Q, Czernuszka J, et al. Prolonged osteogenesis from human mesenchymal stem cells implanted in immunodeficient mice by using coralline hydroxyapatite incorporating rhBMP2 microspheres. *J Biomed Mater Res A*. 2010;92:1256–1264.
38. Shiels S, Oh S, Bae C, et al. Evaluation of BMP-2 tethered polyelectrolyte coatings on hydroxyapatite scaffolds in vivo. *J Biomed Mater Res B Appl Biomater*. 2012;100:1782–1791.
39. Dong X, Wang Q, Wu T, Pan H. Understanding adsorption-desorption dynamics of BMP-2 on hydroxyapatite (001) surface. *Biophys J*. 2007;93:750–759.
40. Mizushima Y, Ikoma T, Tanaka J, et al. Injectable porous hydroxyapatite microparticles as a new carrier for protein and lipophilic drugs. *J Control Release*. 2006;110:260–265.
41. Volkmer E, Drosse I, Otto S, et al. Hypoxia in static and dynamic 3D culture systems for tissue engineering of bone. *Tissue Eng Part A*. 2008;14:1331–1340.
42. Ikeda J, Zhao C, Chen Q, Thoreson AR, An KN, Amadio PC. Compressive properties of cd-HA-gelatin modified intrasynovial tendon allograft in canine model in vivo. *J Biomech*. 2011;44:1793–1796.
43. Akman AC, Tigli RS, Gumusderelioglu M, Nohutcu RM. bFGF-loaded HA-chitosan: a promising scaffold for periodontal tissue engineering. *J Biomed Mater Res A*. 2010;92:953–962.
44. Young S, Patel ZS, Kretlow JD, et al. Dose effect of dual delivery of vascular endothelial growth factor and bone morphogenetic protein-2 on bone regeneration in a rat critical-size defect model. *Tissue Eng Part A*. 2009;15:2347–2362.
45. Sun X, Kang Y, Bao J, Zhang Y, Yang Y, Zhou X. Modeling vascularized bone regeneration within a porous biodegradable CaP scaffold loaded with growth factors. *Biomaterials*. 2013;34:4971–4981.